Testing VSP-based Q-estimation with spherical wave models

Arnim B. Haase and Robert R. Stewart

ABSTRACT

Q-estimation with VSP data from Alberta and Saskatchewan led to the conclusion that stratigraphic effects are a significant part of those estimates. As a first step toward a better understanding of stratigraphic attenuation, we investigate the response to spherical waves of a simple density step model. The Sommerfeld integral is utilized to compute synthetic VSP down-going waves by numerical integration. Q-factors are estimated from these down-going wave fields by applying the spectral ratio method, the analytical signal method, a misfit minimization method adapted from Toverud and Ursin (2005) as well as a modification of the spectral ratio method introduced by Taner and Treitel (2003). We find that at larger depths, away from density steps, all methods recover the model Q-factor quite well. A departure of recovered Q from model Q at shallow depths is noticeable for all methods and is thought to be caused by near-field effects. Q-estimation errors for some methods are found to be considerable in the vicinity of single interfaces investigated. Q-estimates obtained by methods based on spectral ratios appear to be least sensitive to step changes in density values, at least in noise-free situations.

INTRODUCTION

In his introduction to the "*special section – seismic quality factor*" Best (2007) highlights the increased interest in recent years in seismic wave attenuation phenomena and seismic absorption (intrinsic attenuation). He writes, "It could be argued that understanding the physical processes giving rise to absorption is the last barrier to the full realization of the potential of seismic methods". He also mentions the practical difficulties due to restricted bandwidth and poorly constrained multiple scattering as well as geometric spreading losses. The above very nicely sums up our motivation for undertaking the study presented here. Q-estimation utilizing VSP data from different locations on the Canadian Prairies (Haase and Stewart, 2006a; ibid, 2007) led to the conclusion that stratigraphic effects were significant in those estimates. This conclusion is supported by a well-log based 2D elastic wave equation modelling study implementing Virieux's staggered grid finite difference method (Haase and Stewart, 2006b). Figure 1 shows a synthetic VSP from that modelling study and Figure 2 gives a Q-estimate computed from the traces in Figure 1. The trend of this Q-estimate is similar to Q(z) computed from actual VSP data, but there is no intrinsic attenuation in the model. As a first step toward a better understanding of stratigraphic attenuation, we investigate a simple step model in this study. VSP measurements are commonly made with down-hole receivers and their first arrivals are considered to be multiple free. In fact, an entire time zone for upgoing waves following the first arrivals is said to be largely multiple free (after deconvolution) and *corridor stacks* are computed for this zone. However, transmission effects have modified the amplitude behaviour even of isolated down-going wave fields. What is the sensitivity of Q-factors estimated from first arrival amplitudes with respect to transmission coefficients? In a classic paper by O'Doherty and Anstey (1971) the point is made that forward scattering overpowers the true direct wave in seismic reflection measurements of a layered earth. Richards and Menke (1983) show by

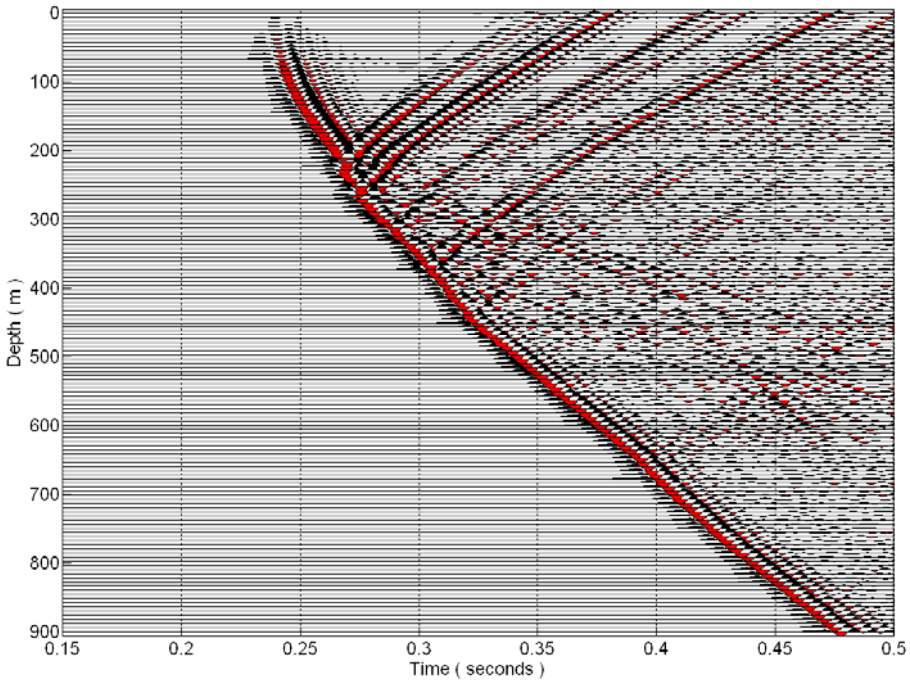

FIG. 1. 2D Velocity-Stress Model VSP based on a Ross Lake well-log (399m offset, displayed is vertical particle velocity).

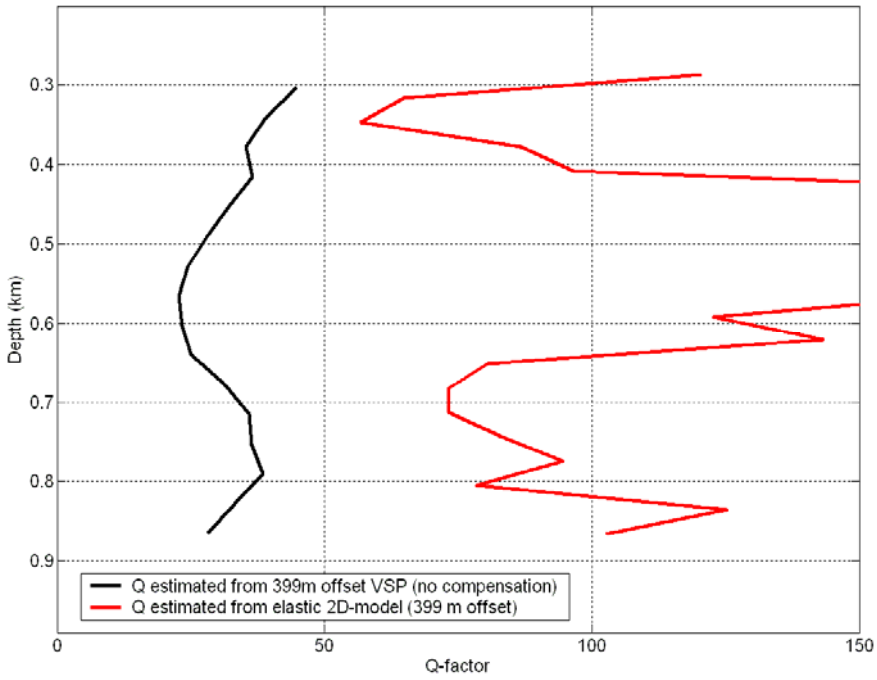

FIG. 2. Quality factor (Q) as determined from Ross Lake VSP data and the model of Figure 1.

numerical experiments that scattering attenuation can be significant and should not be neglected. Mateeva (2003) devotes an entire chapter to *Distortions In VSP Spectral Ratios Caused By Thin Horizontal Layering*. Plane wave analysis is used there to investigate the influence of geology on spectral ratios. By contrast, spherical waves are employed for this contribution. The Sommerfeld integral is utilized to compute synthetic VSP down-going waves by numerical integration. Q-factors are estimated from these down-going wave fields by applying the spectral ratio method, the analytical signal method, a misfit minimization method adapted from Toverud and Ursin (1999) as well as a modification of the spectral ratio method introduced by Taner and Treitel (2003).

THEORY

Johnston and Toksöz (1981) define intrinsic attenuation (Q) as

$$Q = -\frac{\omega E}{(dE/dt)} = -2\pi\frac{W}{\Delta W}, \tag{1}$$

where E is instantaneous energy, dE/dt is the rate of energy loss, W is the elastic energy stored at maximum stress and strain, and ΔW is the energy loss per cycle of a harmonic excitation. The energy E in a wave is proportional to the square of its amplitude or

$$E \sim A^2 \tag{2}$$

giving

$$\frac{dE}{dA} \sim 2A \tag{3}$$

and

$$\frac{dE}{E} = 2\frac{dA}{A} \tag{4}$$

Introducing Equation 4 into Equation 1 gives

$$\frac{1}{Q} = -\frac{dE/dt}{\omega E} = -\frac{dE}{E}\frac{1}{\omega dt} = -\frac{dA}{A}\frac{2}{\omega dt} \tag{5}$$

and

$$\frac{dA}{A} = -\frac{\omega}{2Q}dt \tag{6}$$

Integrating both sides results in

$$\ln(A) + C = -\frac{\omega}{2Q}t \tag{7}$$

and with

$$C = -\ln(A_0) \tag{8}$$

we obtain

$$A(\omega) = A_0 e^{-\left[\frac{\omega t}{2Q}\right]} \tag{9}$$

(see also Aki and Richards, 1980)

In deriving these equations, Q » 1 is assumed, so that the amplitude loss over one wavelength is small. For the developments below, we also assume that attenuation is a linear phenomenon and Fourier-methods can be applied.

The derivation of Q-estimation methods is usually based on the definition of the quality factor Q. For the spectral ratio method (see for example Tonn, 1991) Equations 7 and 8 are the starting point:

$$\ln(A_1) - \ln(A_0) = \ln\left[\frac{A_1(\omega)}{A_0(\omega)}\right] = -\frac{\omega t}{2Q} \tag{10}$$

When applied to VSP-data, t in Equation 10 is the travel time between the two depth stations where A_0 and A_1 are measured. Also present is spherical spreading, so we can write

$$\ln(G_1 A_1) - \ln(G_0 A_0) = \ln\left[\frac{G_1 A_1}{G_0 A_0}\right] = \ln\left[\frac{A_1(\omega)}{A_0(\omega)}\right] + \ln\left[\frac{G_1}{G_0}\right] = -\frac{\omega t}{2Q} \tag{11}$$

The term $\ln[G_1/G_0]$ is a log-spreading ratio which represents a usually ignored intercept. The log-amplitude ratio is a linear function of frequency; Q is calculated from the slope of this curve. For a homogeneous medium, Equation 11 is accurate and Q-factors can be recovered exactly (within numerical accuracy). A change in elastic parameters however, can modify transmitted waves (as well as cause reflections) and alter the frequency response which means spectral ratios are also modified. Aki and Richards (1980) give an equation for the transmitted potential of a two-layer acoustic case (Weyl/Sommerfeld integral approach). The generalization for a layered elastic earth (3D equation for a 1D earth, see for example Ewing et al., 1957) can be written as

$$u_{pp}(\omega) = i\omega e^{-i\omega t} \int_0^{\infty} \prod_{j=2}^{n} \left[\frac{\alpha_j}{\alpha_{j-1}} T_j(p) \right]$$

$$\times \left[\frac{p^2}{\xi_n} J_1(\omega p r) \sin(i_n) - ip J_0(\omega p r) \cos(i_n) \right] e^{i\omega \sum_{k=1}^{n} (\Delta z_k \xi_k)} dp \qquad (12)$$

where $u_{pp}(\omega)$ is the P-wave displacement along the ray at the current receiver and ω,

ω is the frequency in radians,
t is the time,
n is the number of layers from the source down to the current receiver,
α_j is the P-wave velocity in layer j,
$T_j(p)$ is the Zoeppritz transmission coefficient from layer j-1 to layer j,
p is the horizontal slowness,
ξ_n is the vertical slowness of layer n,
J_0 and J_1 are zero and first order Bessel functions of the first kind,
r is the range (horizontal offset between source and receivers), and
i_n is the ray angle in layer n (at the current receiver).

A number of frequency points are computed at every receiver location (depth **z**) according to the desired bandwidth/wavelet. The time-domain wavefield can then be obtained by inverse Fourier transforming.

Note that Equation 12 models transmitted waves only and, because of the Bessel functions, spherical spreading is included. Also modelled are near-field and far-field effects.

FAR-FIELD VERSUS NEAR-FIELD IN A HOMOGENEOUS MEDIUM

Zero-offset synthetic VSP traces computed with Equation 12 for a homogeneous situation are displayed in Figure 3. The parameters for this earth model are α=2000m/s, β=879.88m/s, ρ=2400kg/m^3 and Q_p=100. Amplitude decay with increasing depth is clearly visible. Also notice the phase rotation between shallower and deeper traces. As the near-field decays with $1/r^2$ (in contrast to 1/r for the far-field, see Aki and Richards, 1980) its influence quickly disappears with increasing depth. At shallow depths, where the near-field predominates, we can expect time-domain Q-estimation methods to underestimate Q (overestimate attenuation) because of the $1/r^2$ amplitude decay. Figure 4 shows far-field log magnitude spectra as generated with Equation 12 for depths from 175m to1227m. The zero-phase (non-causal) Ormsby wavelet employed for these computations has the parameters 5/15-80\100 Hz. Q-factor recovery in this band is expected to be almost perfect because spectral ratio methods are derived for these circumstances with linear log ratio slopes. The deeper the receiver, the steeper the log magnitude curve. Note that all spectra in Figures 4 and 5 are normalized to the same zero dB maximum but the plotting scales differ between the Figures. The near-field equivalent to Figure 4, now for depths from 15.2m to 60.9m, is shown in Figure 5. For the near-field

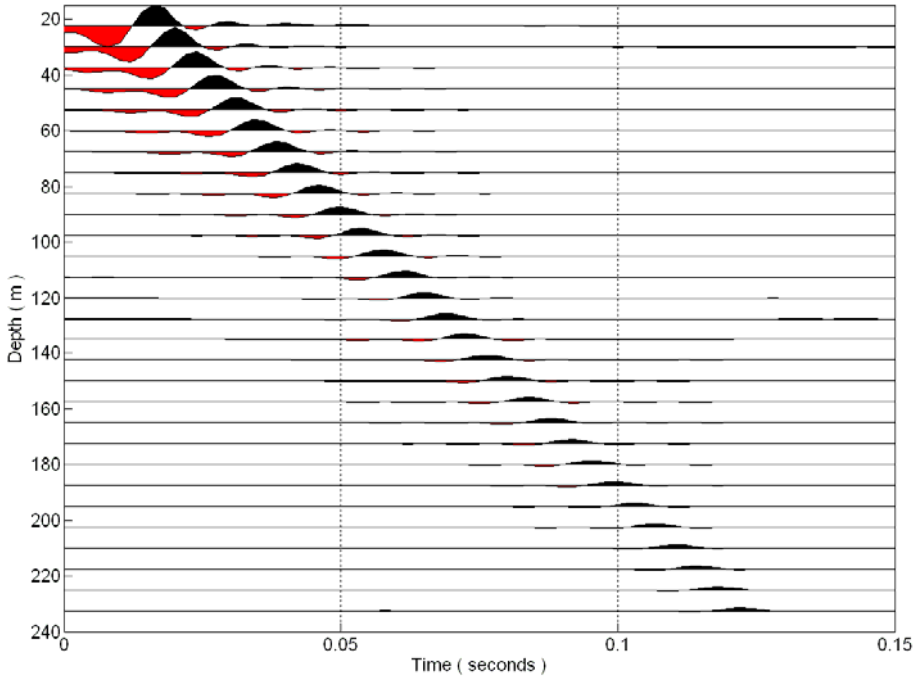

FIG. 3. Zero offset synthetic VSP computed with Equation 12 for a zero-phase (non-causal) 5/15-80\100Hz Ormsby wavelet.

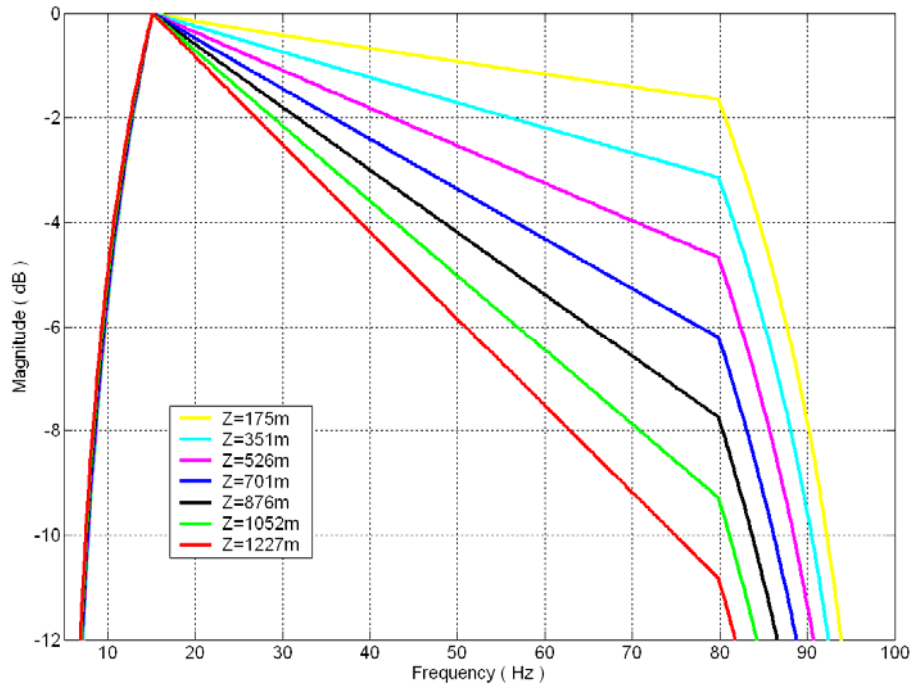

FIG. 4. Far-field magnitude spectrum for depth range from 175m to 1227m (0dB scaling).

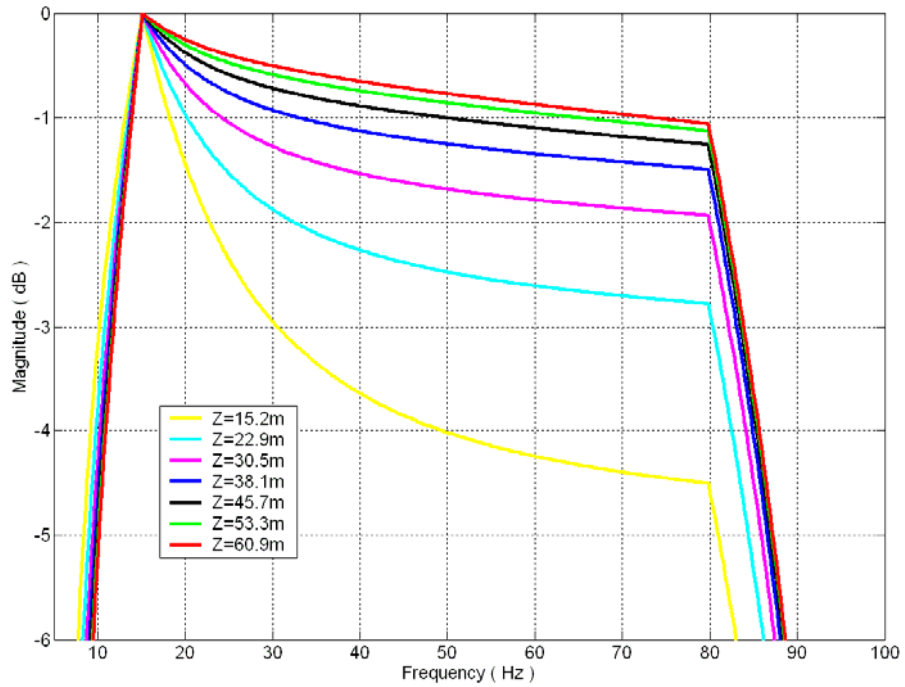

FIG. 5. Near-field magnitude spectrum for depth range from 15.2m to 60.9m. The downgoing wavefield appears to be gaining (relative) high frequency strength with depth (0dB scaling).

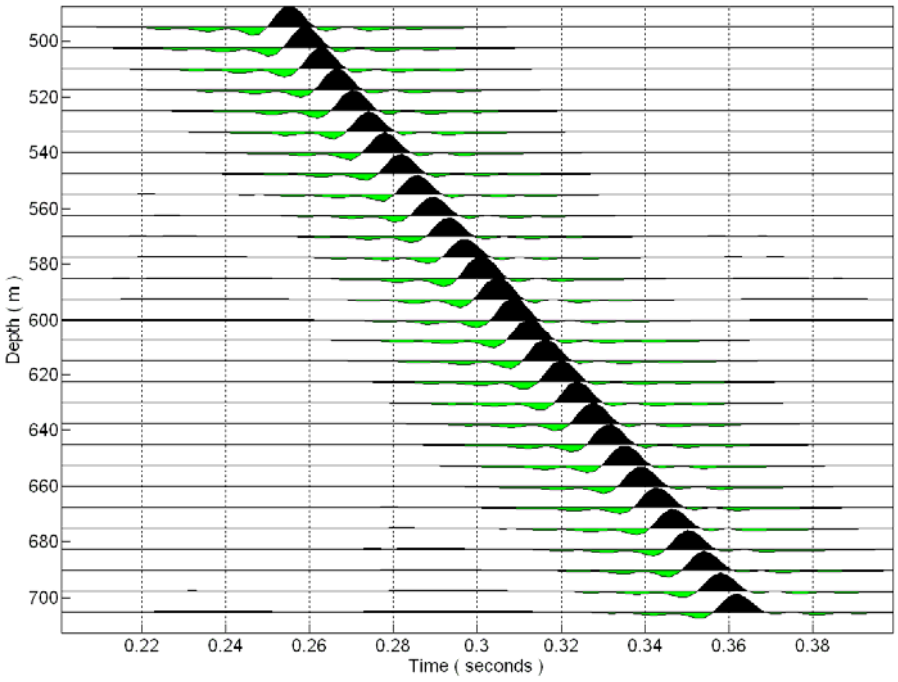

FIG. 6. Selected traces of half-density-step model.

the slopes show an opposite trend: the shallower the receiver, the steeper the log magnitude curve. The only exception can be seen for the deepest receivers (at 53.3m and 60.9m depths) above 40Hz or 50Hz. Q-estimation leads to negative Q-factors near the source and large positive Q some distance away in the near-field where the slope trend is reversed but the log magnitude curves are still almost parallel. As far-field conditions are approached the estimated Q converges with the model Q. It is interesting to note that this kind of *near-field behavior* has also been observed when estimating Q from actual VSP data (Haase and Stewart, 2006a; ibid, 2007). Where does the near-field stop and the far-field begin? Aki and Richards (1980) use the term "many wavelengths" when describing the distance from source points to where far-field approximations start to be accurate. Common practice is to assume "several wavelengths" are sufficient for far-field approximation accuracy (E. Krebes, personal communication). It would be interesting to compute the difference between "exact" and "far-field only" of the wavefield to obtain a near-field estimate, but that is a topic for a separate report.

THE DENSITY CHANGE MODEL

The parameters for this earth model are α=2000m/s, β=879.88m/s, ρ=2400kg/m^3 and Q_p=100. At approximately 580m depth an abrupt density change to A) 1200kg/m^3 (half density step) and to B) 4800kg/m^3 (twice density step) is introduced. The traces for the density step model of case A) (a density decrease) computed with Equation 12 are plotted in Figure 6 for the vicinity of the density step location at approximately 580m depth. A density decrease implies a decrease in acoustic impedance which leads to an increase in particle displacement. Indeed, close inspection of Figure 6 reveals an amplitude increase at depths exceeding the density step location at about 580m. Superimposed at all depths is the amplitude decay caused by spherical spreading. The move out between traces is linear (there is no variation with depth) because of constant velocities. Note the ringing typical for Ormsby wavelets. Figure 7 is the equivalent to Figure 6 computed for case B) (a density increase). A density increase results in an acoustic impedance increase which means particle displacement is decreased. As expected, maximum trace amplitudes in Figure 7 are decreasing at depths exceeding the density step location at about 580m. Amplitude decay because of spherical spreading is present but barely visible. Figures 6 and 7 are plotted at different scales to highlight trace-to-trace amplitude changes.

DENSITY CHANGE AND THE SPECTRAL RATIO METHOD

Next, the spectral ratio method (SRM) given in Equation 11 is applied to the density change models introduced in the previous section. Figure 8 shows the Q-factors estimated from the computed model traces. These Q(z) curves depend on smoother lengths and depth intervals used for estimation with the spectral ratio method. In this case the amplitude spectra of three neighbouring traces are averaged and the estimation depth interval is Δz=38m.

Away from the density step the model Q-factor of 100 is quite well recovered in Figure 8. The departure of recovered Q from model Q at depths shallower than approximately 200m in all Q(z) displays is thought to be caused by near-field effects as explained above (see Figure 5 for the slope behaviour of near-field log magnitude spectra). At the density step decrease in Figure 8 SRM is seen to firstly underestimate Q and then secondly overestimate Q as the analysis window slides across the discontinuity.

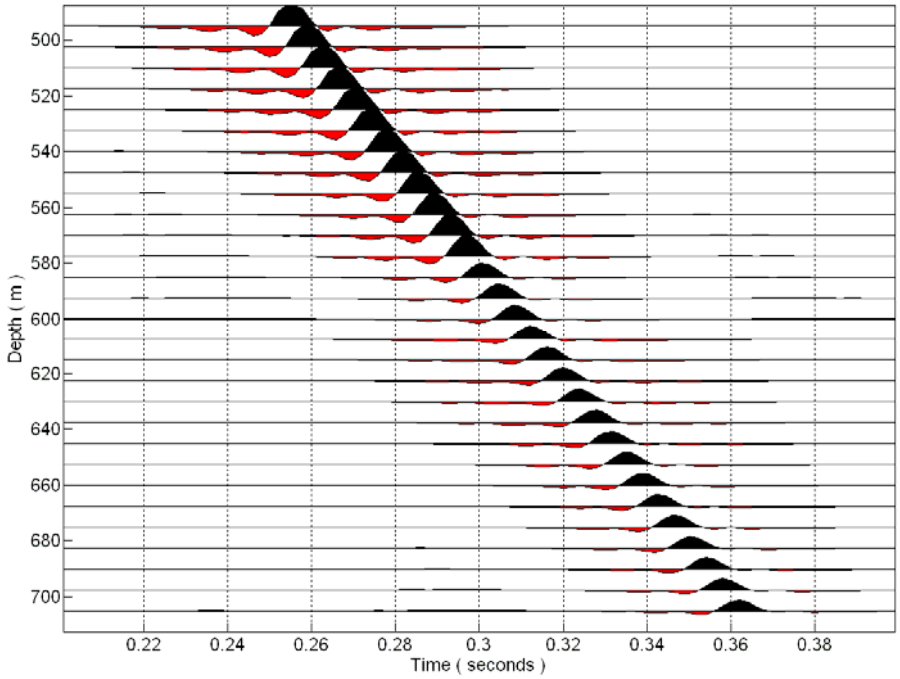

FIG. 7. Selected traces of twice-density-step model.

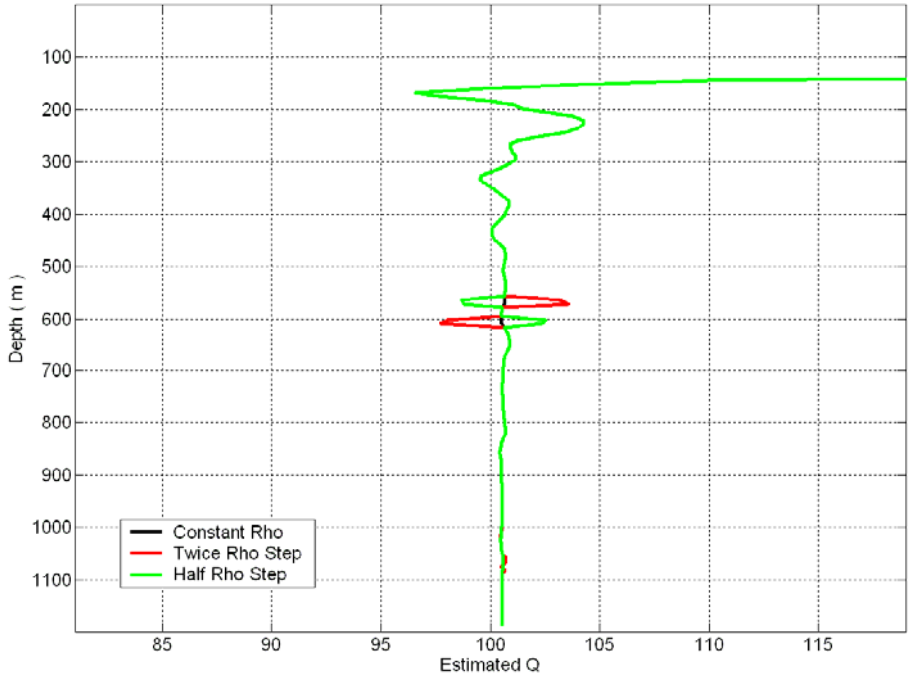

FIG. 8. Q-estimate by spectral ratio method (density step model).

For a density step increase the situation is reversed: We see in Figure 8 that Q is overestimated first as the analysis window reaches the discontinuity and is followed secondly by an underestimate. Pulse width, pulse height and pulse separation of these error pulses are controlled by smoother lengths and analysis window size (depth interval Δz). Note that these error pulses represent only a few percent Q-estimation error for SRM even though the density change is much larger (50% down and 100% up).

DENSITY CHANGE AND THE ANALYTICAL SIGNAL METHOD

The analytical signal method (ASM) estimates the quality factor (Q) from the decay of instantaneous amplitudes with depth (see Tonn, 1991). Figure 9 shows an ASM Q-estimate obtained from the homogeneous VSP model traces displayed in Figure 3. Because of the near-field decay with $1/r^2$, shallow depth Q-factors are underestimated as anticipated. The far-field Q-estimate approaches the model Q-factor of 100 nicely but the ripple visible in the Q(z) curve is puzzling at first glance. In Figure 10 the same curve is plotted at a larger scale. There is an obvious periodicity with depth which brings to mind the maximum instantaneous amplitude picking required for this ASM algorithm. Because of a finite time sampling rate there will not always be a sample right at the maximum amplitude of every trace and this off-maximum sampling could cause the observed trace-to-trace periodicity. The sample interval of the traces in Figure 3 is 2ms. Decreasing this sample interval to 1ms as well as re-computing traces and Q(z) leads to the green curve in Figure 11. This appears to be a step in the right direction as the Q(z) curve ripple is approximately halved for a 1ms sample interval when compared to the 2ms equivalent. The blue curve in Figure 11 is obtained by frequency-domain interpolation of 1ms traces to a 1/8ms sample interval and Figure 12 shows those curves re-plotted at the original scale of Figure 9. A sample interval of 1/8ms appears acceptable for out purposes here.

Next, the analytical signal method is applied to the density step-increase model introduced and utilized in previous sections. The Q(z)-ripple of the result in Figure 13 is not unexpected since the traces of this particular model are computed with a 2ms sample interval. However, what comes as a surprise is the size of the Q-estimation error at approximately -60% when the density is increased by 100%. The ASM-technique (time-domain) is considerably more sensitive to amplitude disturbances than the SRM-approach (frequency-domain). Therefore, for further ASM-testing, we reduce the density step size to ±5% (and reduce the sample interval to 1/8ms). Q-estimates for model VSPs with a density step to 95% and a density step to 105% are shown in Figure 14. Note the density step location is at approximately 580m depth. For a decrease in density, Q is overestimated and vice versa. There is a Q-estimation error for the entire depth-range spanned by the combination of smoother length and analysis window. Even though the far-field Q-estimate closely approaches the model Q-factor of 100, the near-field influence on the Q-estimate extends further in depth for the ASM-algorithm than it does for the SRM-technique.

DENSITY CHANGE AND THE METHOD BY TOVERUD AND URSIN

Toverud and Ursin (2005) use a normalized misfit function to compare seismic attenuation models. Given an attenuation model, this misfit function can be minimized as part of an optimization loop searching for a “best-fit” Q-factor and a “best-fit” velocity. Thus amplitude and phase information are included in the Q-estimation. In deriving the

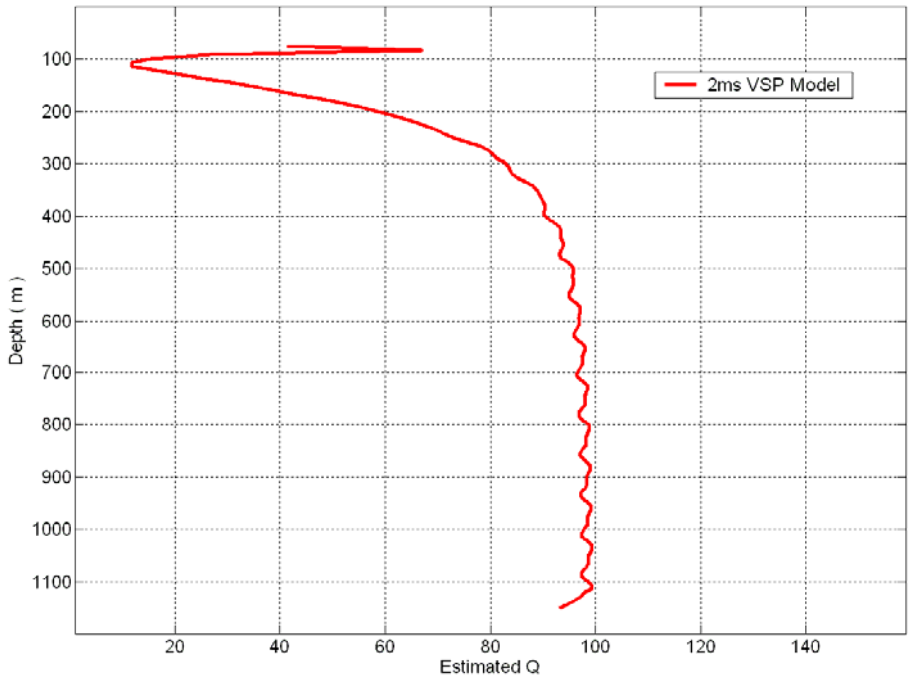

FIG. 9. ASM Q-estimate of 2ms homogeneous VSP model traces in Figure 3.

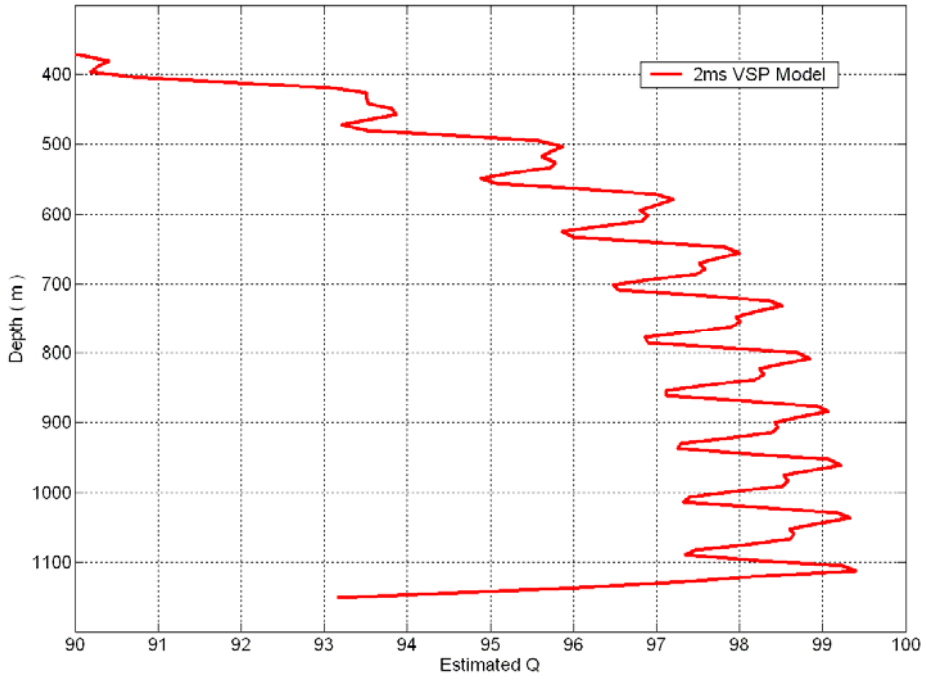

FIG. 10. Same ASM Q-estimate as Figure 9 plotted at larger scale.

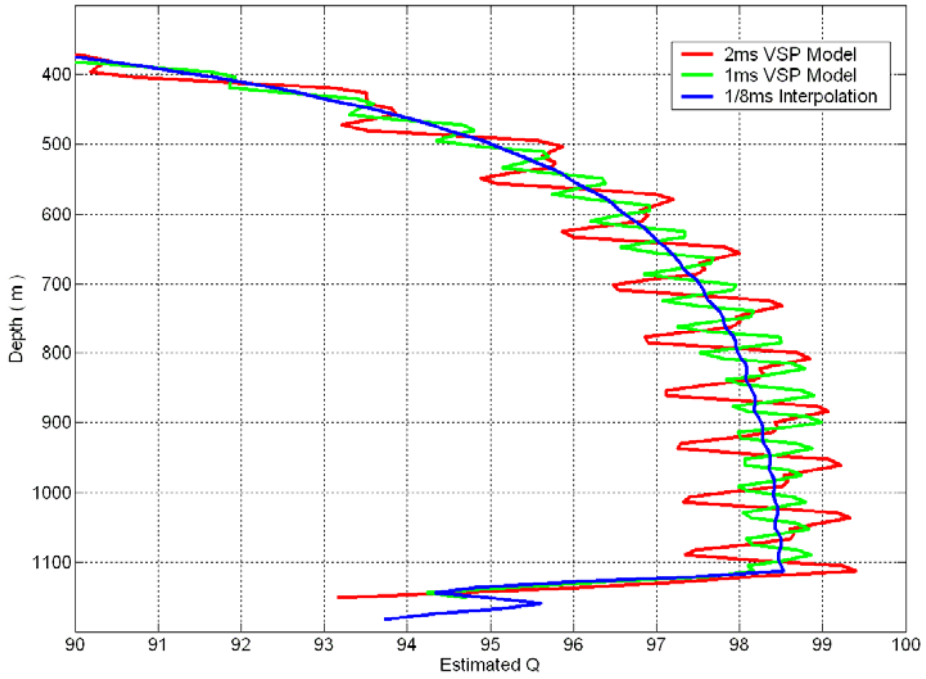

FIG. 11. Sample interval tests for analytical signal method.

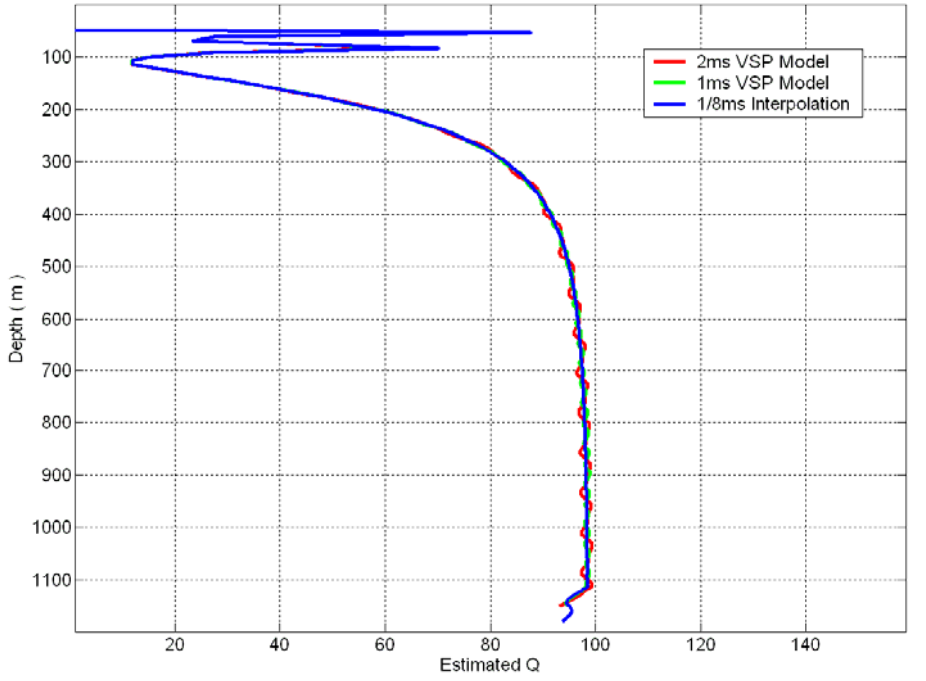

FIG. 12. ASM sample interval tests of Figure 11 re-plotted at scale of Figure 9.

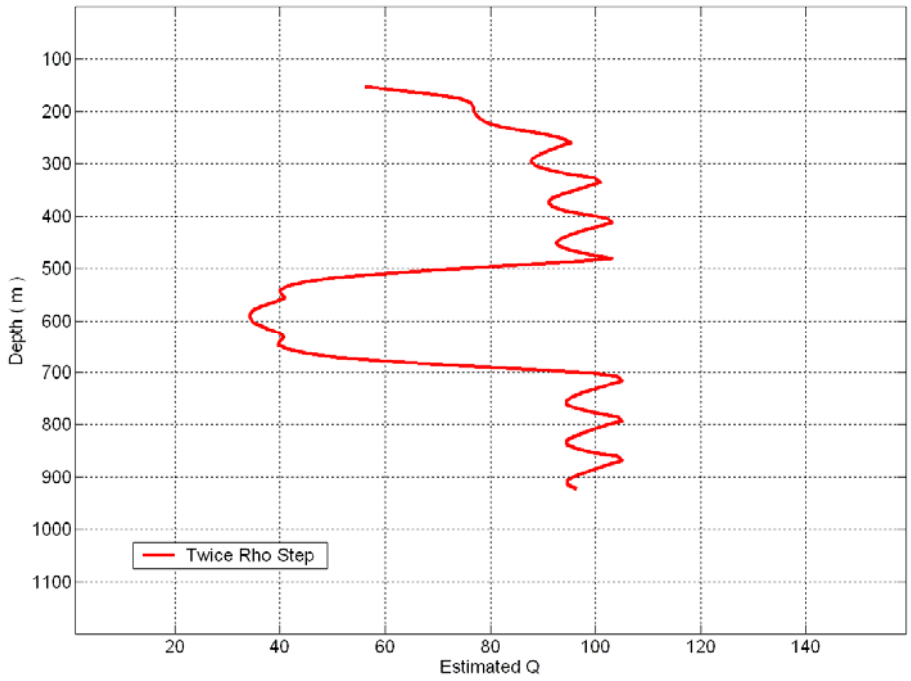

FIG. 13. ASM Q-estimate of 2ms twice-density-step model.

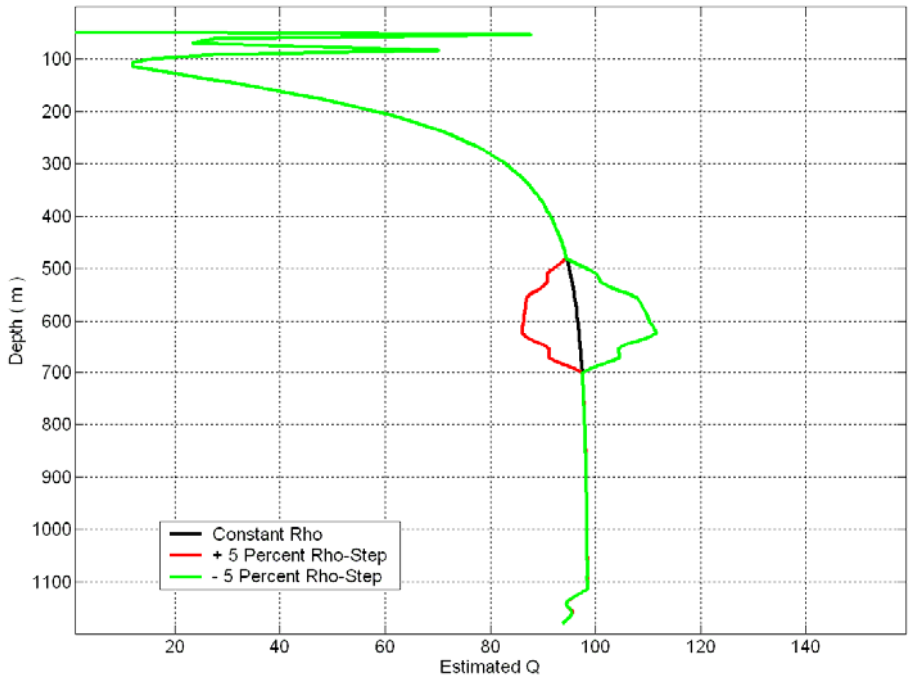

FIG. 14. ASM Q-estimate of +/- 5% density-step model (1/8ms).

misfit function it is assumed that, within a finite number of designated homogeneous layers, velocities and attenuation do not change. Squared error contributions are accumulated (summed) for all receivers within a layer as well as for all discrete frequencies in the data frequency band and then normalized (Toverud and Ursin, 2005):

$$\Delta E_N = \frac{\sum_j \sum_\omega | P(z_j,\omega) - \hat{P}(z_j,\omega) |^2}{\sum_j \sum_\omega | P(z_j,\omega) |^2} \tag{13}$$

$P(z_j,\omega)$ is the date at the j^{th} receiver of the current layer following a Fourier transform into the frequency domain. The modelled data as function of depth z and frequency ω is estimated by

$$\hat{P}(z,\omega) = \frac{P(z_0,\omega)L(z_0)}{L(z_0)+\Delta L(z)} e^{j\omega\Delta\tau(z,\omega)} \tag{14}$$

where $\Delta\tau(z,\omega)$ is the incremental travel time in the current layer, $P(z_0,\omega)$ is the Fourier transformed data at the top of the current layer at z_0, $L(z_0)$ is the approximated relative geometrical spreading down to the top of the current layer given by

$$L(z_0) = \int_0^{z_0} c_p(\zeta,\omega_r)\, d\zeta \tag{15}$$

and $\Delta L(z)$ is the incremental relative spreading in the current layer approximated by

$$\Delta L(z) = c_p(\omega_r)(z - z_0) \tag{16}$$

with $c_p(\omega_r)$ representing phase velocity at a reference frequency ω_r (constant within layers but depth dependent in the overburden). The frequency-dependent-velocity equation used here for the attenuation modelling step is taken from Aki and Richards (1980, page 182):

$$v(\omega) = v_{ref}\left(1 + \frac{\ln(\omega/\omega_{ref})}{\pi Q} - \frac{i}{2Q}\right) \tag{17}$$

Next we apply Toverud and Ursin's misfit minimization method to the *density step to 95%* model VSP and the *density step to 105%* model VSP as introduced previously for the ASM-tests. The estimated *best-fit* Q-factors are displayed in Figure 15. We see immediately that Q-estimation error size and sensitivity to density change are similar to

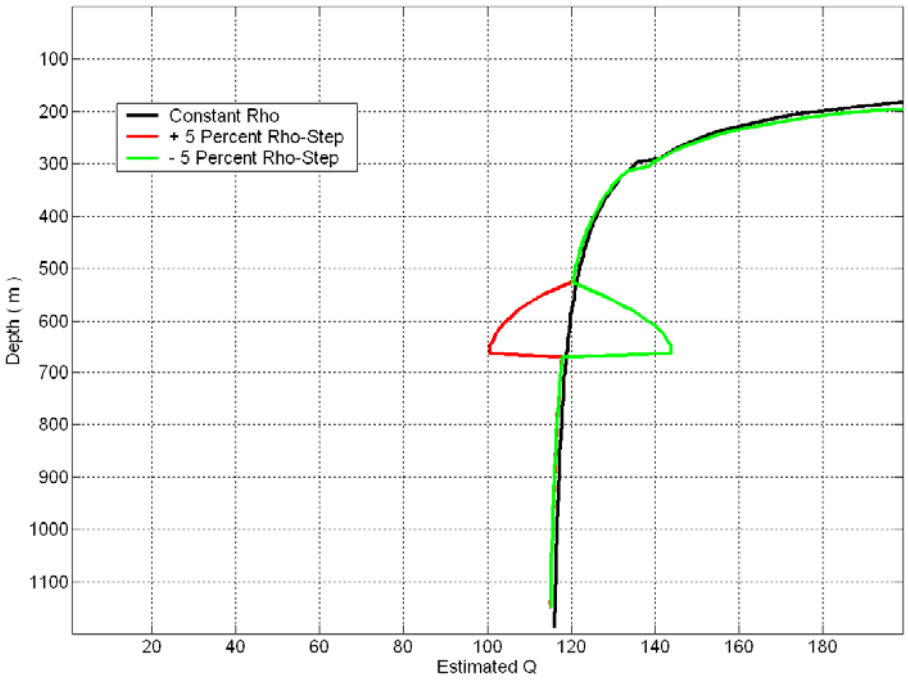

FIG. 15. Q-estimate by Toverud and Ursin's method (density step model).

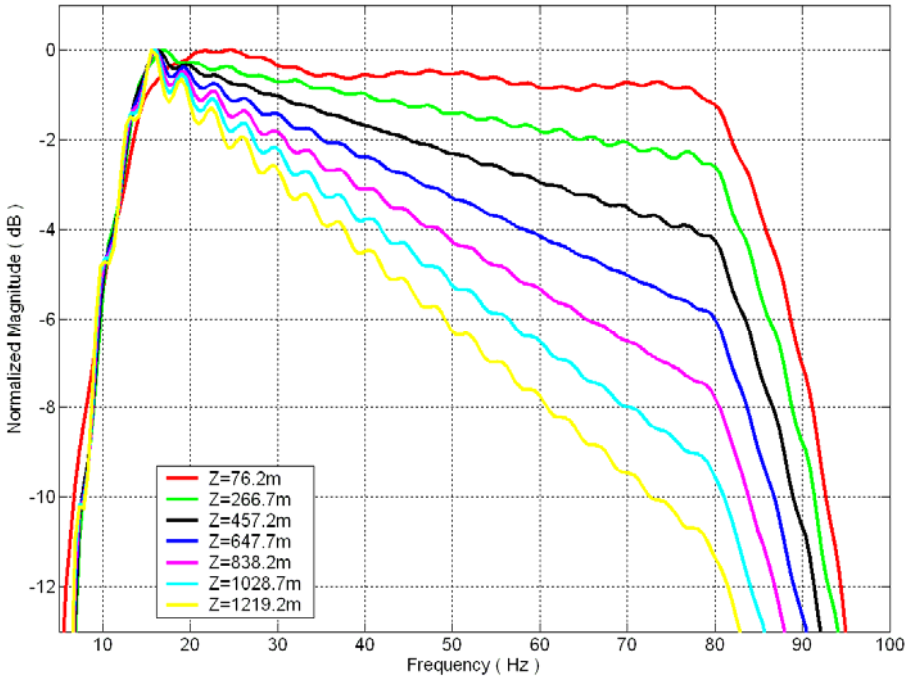

FIG. 16. Magnitude spectrum of minimum phase wavelet for depth range from 76m to 1219m.

ASM-results (compare to Figure 14) with two notable differences: Firstly, the near-field responses of the Q-estimates shown in Figure 15 are more like SRM near-field Q-estimates (Figure 8) that increase toward shallower depths. Secondly, the estimated Q in Figure 15 does not approach the model Q as closely as the other methods do when far-field conditions are reached. Occasionally, optimization routines find a local minimum, a condition that can be tested by changing the starting values for the procedure. In this case the estimated Q(z) is independent of the starting value of Q. However, the far-field bias of Q and the Q-estimation error size at the density step are sensitive to the choice of reference frequency in Equation 17. Figure 15 is computed with the same value of ω_r as is used to generate the synthetic VSP. The positive bias on far-field Q-estimates looks like an overcompensation of the spherical spreading correction. The approximations used for spherical spreading correction are given in Equations 15 and 16. Their dependence on the reference frequency ω_r explains the sensitivity of the far-field Q-estimation bias to ω_r.

DENSITY CHANGE AND THE METHOD BY TANER AND TREITEL

Taner and Treitel (2003) suggested a modification of the standard spectral ratio method (SRM) based on minimum phase *wavelets* estimated from designated data zones. Their method (TTM) proceeds by, firstly, computing auto-correlations for these zones. Secondly, a minimum phase *inverse* of each auto-correlation is calculated by applying Levinson's recursion. Thirdly, the inverse of step 2 is computed which is a stable operation because of the minimum phase character. Lastly, Q is estimated from two minimum phase *wavelets* with the approach of the standard spectral ratio method. According to Taner and Treitel (2003) their method is less prone to the influence of zeros on or near the unit circle in the Z-plane (notches) because minimum phase wavelets cannot have zeros on the unit circle. Figure 16 displays magnitude spectra of minimum phase wavelets computed from first arrivals of the synthetic VSP (Figure 3). We no longer have the straight lines of Figure 4 (standard SRM) but neither do Taner and Treitel (2003). Their Figure 5 shows similar "ripples" of spectral ratios. As required for the standard SRM, we calculate log spectral ratios next. Figure 17 shows log spectral ratios computed from magnitude spectra displayed in Figure 16. Not unexpectedly so, magnitude spectra noise "ripples" are propagated to the log ratios. This fact does not prevent us from straight line fitting, however, even for the shallowest ratio at 76m depth which we reject out of hand as "near-field contaminated". Q(z) estimated from the fitted straight lines (according to Equation 11) is plotted in Figure 18 for the same density step VSP-model cases as investigated with standard SRM techniques (Figure 8). When comparing Figures 8 and 18 we notice general agreement between SRM and TTM Q(z). This is expected because we did not model any spectral notches with our synthetic VSP. Looking at the details, however, reveals an increase of Q-estimation errors of up to several percent for the Taner and Treitel technique. For a real VSP data comparison between TTM and SRM see Haase and Stewart (2007).

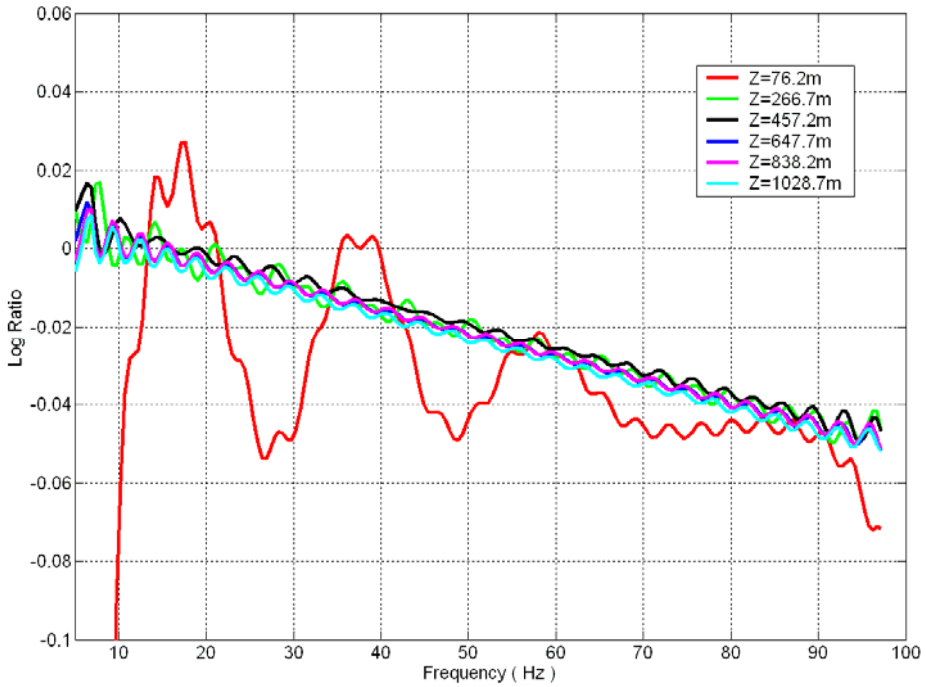

FIG. 17. Log spectral ratios computed from minimum phase wavelets (Taner and Treitel).

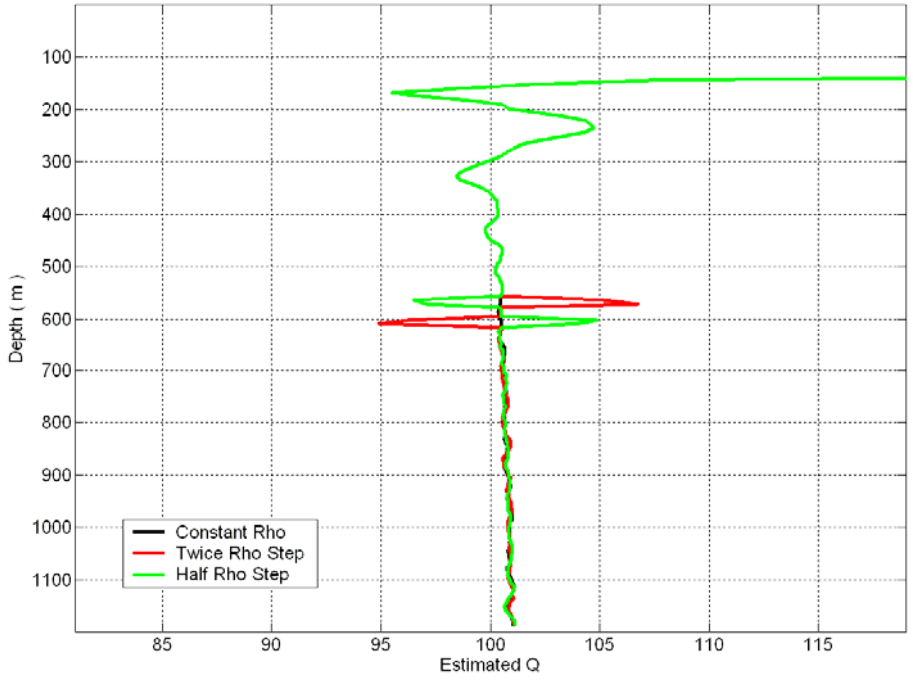

FIG. 18. Q-estimate by Taner and Treitel's method (density step model).

CONCLUSIONS

Away from density steps, at larger depths, all methods recover the model Q-factor of 100 quite well. The largest departure is observed for the "Q-estimation through misfit minimization" method (Toverud and Ursin, 2005) which we think is caused by using only reference velocities for computing the incremental relative geometrical spreading (Equation 16).

The departure of the recovered Q from the model Q at shallow depths is noticeable for all methods and is thought to be caused by near-field effects. Where the near-field predominates we can expect time-domain Q-estimation methods to *underestimate* Q because of the $1/r^2$ amplitude decay. The specific slope behaviour of magnitude spectra observed for decreasing depths leads to *overestimated* Q for spectral ratio methods and even to negative Q near the source. When estimating Q from actual VSP data (Haase and Stewart, 2006a; ibid, 2007) the same kind of *near-field behaviour* is observed.

Q-estimates obtained by methods based on spectral ratios appear to be least sensitive to step changes in density values, at least in noise-free situations. For the analytical signal method and the misfit function minimization technique density-step responses of Q(z) are somewhat smeared out because of depth averaging.

If velocities and densities are known, we expect transmission loss compensation to reduce far-field Q-estimation errors. We anticipate a modelling approach is required to reduce near-field transmission errors.

ACKNOWLEDGEMENTS

Support by the CREWES team and its industrial sponsorship is gratefully acknowledged.

REFERENCES

Aki, K.T., and Richards, P.G., 1980, Quantitative Seismology: Theory and Methods: Vol. 1, W.H. Freeman and Co.

Best, A.I., 2007, Introduction to Special section – Seismic Quality Factor: Geophysical Prospecting, **55**, 607-608.

Ewing, W.M., Jardetzky, W.S., and Press, F., 1957, Elastic Waves in Layered Media: McGraw-Hill, New York.

Haase, A.B., and Stewart, R.R., 2006a, Estimating Q from VSP data: Comparing spectral ratio and analytical signal methods: CREWES Research Report, **18**.

Haase, A.B., and Stewart, R.R., 2006b, Stratigraphic attenuation of seismic waves: CREWES Research Report, **18**.

Haase, A.B., and Stewart, R.R., 2007, VSP-based Q-estimation at Pike's Peak: CREWES Research Report, **19**.

Johnston, D.H., and Toksöz, M. N., 1981, Seismic wave attenuation: Society of Exploration Geophysicists, page 2.

Mateeva, A.A., 2003, Thin horizontal layering as a stratigraphic filter in absorption estimation and seismic deconvolution: Ph.D. Thesis, Colorado School of Mines.

O'Doherty, R.F., and Anstey, N.A., 1971, Reflections on amplitudes: Geophysical Prospecting, **19**, 430-458.

Richards, P.G., and Menke, W., 1983, The apparent attenuation of a scattering medium, BSSA, **73**, 1005-1021.

Taner, M.T., and Treitel, S., 2003, A robust method for Q estimation: **73rd** Annual SEG Meeting Expanded Abstracts, Paper IT3.6, 710-713.

Tonn, R., 1991, The determination of seismic quality factor Q from VSP data: A comparison of different computational methods: Geophys. Prosp., **39**, 1-27.

Toverud, T., and Ursin, B., 2005, Comparison of seismic attenuation models using zero-offset vertical seismic profiling (VSP) data: Geophysics, **70**, F17-F25.